ORIGINAL ARTICLE

Children's Urinary Environmental Carbon Load

A Novel Marker Reflecting Residential Ambient Air Pollution Exposure?

Nelly D. Saenen[1]*, Hannelore Bové[2,3]*, Christian Steuwe[3], Maarten B. J. Roeffaers[3], Eline B. Provost[1], Wouter Lefebvre[4], Charlotte Vanpoucke[5], Marcel Ameloot[2], and Tim S. Nawrot[1,6]

[1]Centre for Environmental Sciences and [2]Biomedical Research Institute, Hasselt University, Hasselt, Belgium; [3]Centre for Surface Chemistry and Catalysis and [6]Department of Public Health and Primary Care, Leuven University, Leuven, Belgium; [4]Flemish Institute for Technological Research, Mol, Belgium; and [5]Belgian Interregional Environment Agency, Brussels, Belgium

ORCID IDs: 0000-0002-3226-089X (N.D.S.); 0000-0001-7185-3746 (H.B.); 0000-0002-0888-2488 (M.A.).

Abstract

Rationale: Ambient air pollution, including black carbon, entails a serious public health risk because of its carcinogenic potential and as climate pollutant. To date, an internal exposure marker for black carbon particles that have cleared from the systemic circulation into the urine does not exist.

Objectives: To develop and validate a novel method to measure black carbon particles in a label-free way in urine.

Methods: We detected urinary carbon load in 289 children (aged 9–12 yr) using white-light generation under femtosecond pulsed laser illumination. Children's residential black carbon concentrations were estimated based on a high-resolution spatial temporal interpolation method.

Measurements and Main Results: We were able to detect urinary black carbon in all children, with an overall average (SD) of 98.2×10^5 (29.8×10^5) particles/ml. The urinary black carbon load was positively associated with medium-term to chronic (1 mo or more) residential black carbon exposure: $+5.33 \times 10^5$ particles/ml higher carbon load (95% confidence interval, 1.56×10^5 to 9.10×10^5 particles/ml) for an interquartile range increment in annual residential black carbon exposure. Consistently, children who lived closer to a major road (≤160 m) had higher urinary black carbon load (6.93×10^5 particles/ml; 95% confidence interval, 0.77×10^5 to 13.1×10^5).

Conclusions: Urinary black carbon mirrors the accumulation of medium-term to chronic exposure to combustion-related air pollution. This specific biomarker reflects internal systemic black carbon particles cleared from the circulation into the urine, allowing investigators to unravel the complexity of particulate-related health effects.

Keywords: urine; carbon load; biomarker; air pollution; black carbon

Current ambient outdoor air pollution is responsible for 4.2 million premature deaths worldwide (1), ranked within the top 10 of important risk factors for public health. Children are especially vulnerable to the detrimental effects of air pollution and have for the same ambient concentrations a higher internal dose compared with adults because of their higher respiratory rate. Combustion-related particulate matter (PM) air pollution, including black carbon, is associated in early life with lower birth weight (2), decreased

(Received in original form April 21, 2017; accepted in final form July 6, 2017)

*These authors contributed equally.

Funded by the European Research Council (ERC-2012-StG 310898), the Interuniversity Attraction Poles Program (P7/05) initiated by the Belgian Science Policy Office, and the Flemish Scientific Research Foundation (G082113/11ZB115N/12R6315N/G073315N).

Author Contributions: T.S.N. designed the COGNAC (Cognition and Air Pollution in Children) study. H.B., M.A., C.S., and M.B.J.R. developed the protocol for measuring urinary carbon load by femtosecond pulsed laser illumination. H.B. and N.D.S., under the supervision of M.A., performed the urinary carbon analysis. H.B., C.S., and M.B.J.R. conducted the calibration experiments on the urine. N.D.S. and E.B.P. recruited the study population and developed the exposure matrices, with input from C.V and W.L. N.D.S. performed the statistical analysis, with guidance from T.S.N. N.D.S. and H.B. wrote the first draft of the manuscript, with the help of M.A. and T.S.N. All authors were involved in data interpretation and critical revision of the manuscript.

Correspondence and requests for reprints should be addressed to Tim S. Nawrot, Ph.D., Centre for Environmental Sciences, Hasselt University, Agoralaan Building D, 3590 Diepenbeek, Belgium. E-mail: tim.nawrot@uhasselt.be

This article has an online supplement, which is accessible from this issue's table of contents at www.atsjournals.org

Am J Respir Crit Care Med Vol 196, Iss 7, pp 873–881, Oct 1, 2017

Originally Published in Press as DOI: 10.1164/rccm.201704-0797OC on July 7, 2017
Internet address: www.atsjournals.org

At a Glance Commentary

Scientific Knowledge on the Subject: Ambient air pollution, including black carbon, entails a serious public health risk because of its carcinogenic potential and as climate pollutant. Different experimental studies have demonstrated that ultrafine particles can translocate from the lung into the systemic circulation, although the issue of particle translocation in humans is still controversial. To date, an internal exposure marker for black carbon particles that have cleared from the circulation in the urine does not exist.

What This Study Adds to the Field: This is the first time that environmental carbon in urine of children is identified, showing the ubiquity of this environmental pollutant. Our method is based on nonincandescence-related white-light generation under femtosecond illumination, which is a label-free and biocompatible imaging technique. Urinary carbon load can be used as an internal exposure marker for medium-term up to chronic combustion-related air pollution and will assist in unravelling the complexity of ultrafine particles–related health effects.

cognitive function in children (3, 4), impaired cognitive aging (5), increased cardiovascular morbidity and mortality (6, 7), and respiratory diseases (8) and lung cancer (9) in adult life. Three hypotheses are formulated to rationalize these findings: (*1*) particles produce pulmonary oxidative stress and inflammation with a systemic release of cytokines (7), (*2*) the smallest particles translocate from the lungs into the circulation with effects in different organ systems, and (*3*) particles interact with pulmonary receptors or nerves with effects via the autonomic nervous system (10). Experimental studies on animals have shown that a substantial fraction of intratracheally introduced ultrafine particles could translocate into the systemic circulation (11), and even may translocate via the olfactory nerve to the brain when deposited in the nose (12). However, in humans the subject of particle translocation is still under debate because studies have failed to find a considerable fraction of inhaled particles translocated into the circulation. Furthermore, the clinical significance of how these ultrafine particles contribute to health effects remains unclear.

Although some air pollution associations are established as causal (7), risks might be considerably underestimated because of exposure misclassification. In most epidemiologic studies, the exposure to PM air pollution, including black carbon, is not measured at the individual or time-activity pattern level. Instead, spatial temporal models are used, which basically use land cover data that are based on multiple primary sources (i.e., road networks, line and point locations of potential sources, building density) to estimate the daily residential exposure values (13, 14), which results in incomplete information about residential mobility. In these studies, the bulk of exposure measurement error, which is typically "Berkson-like," lead to unbiased but more variable health effect estimates (15). Despite increased understanding of the health consequences of combustion-related air pollution, a critical barrier to progress in the field is limited ability to monitor adequately personalized exposure over the life course. To overcome these shortcomings, we postulated the translocating nature of black carbon particles from the circulation into the urine so that these particles in urine form a biomarker reflecting exposure. Within this framework, we detected and quantified black carbon particles in urine of 289 children living in the northern part of Belgium with relatively low annual ambient black carbon concentrations in the study area ranging from 1.07 to 1.96 $\mu g/m^3$.

Methods

Calibration Experiments for Black Carbon Detection in Urine

In this research, we used a label-free and biocompatible imaging technique based on the nonincandescence-related white-light generation potential of carbonaceous particles under femtosecond illumination (16). Summarized, the heterogeneous and absorptive (dark color) nature of carbonaceous particles gives rise to the white-light phenomenon. For the signal to occur, these two conditions should explicitly be fulfilled. Therefore, (*1*) the possible contribution of any noncarbonaceous material (except for nobel metals, they are able to generate plasmons) is excluded, because they do not comply with the aforementioned conditions; (*2*) carbon-containing materials, such as endogenous structures with carbon backbones, do not generate the white-light because they do not contain multiple absorbing sites; and (*3*) the material generating this signal should be in particle form for exhibiting the heterogeneity and absorptive character.

Here, several experiments were conducted to assess the potential for cross-reactivity or to assess specificity more generally. First, we validated and calibrated the application method for urine imaging using artificial urine. This artificial urine solution was imaged under identical imaging conditions as for analyzing the "real" urine samples, to check for any signal coming from, for example, urinary salt crystals. Second, background signals from naturally present carbonaceous particles in the air and detection chambers were checked by measuring empty Ibidi wells (Ibidi GmbH, Planegg, Germany). Third, cross-reactivity from the most structurally and chemically resembling particles available, named silica particles (17), was checked under identical imaging conditions. Fourth, cross-reactivity from other carbonaceous materials was checked by measuring carbon nanotubes. Fifth, Raman spectroscopy measurements were executed on dried urine samples. For details *see* the online supplement.

Optimized Experimental Protocol for Black Carbon Detection in Urine

The carbonaceous particles in the urine samples were analyzed and images collected using a Zeiss LSM510 META NLO (Carl Zeiss, Jena, Germany) mounted on an Axiovert 200 M equipped with a two-photon femtosecond pulsed laser (MaiTai DeepSee; Spectra-Physics, Mountain View, CA). A detailed description of the set-up and imaging protocol can be found in the online supplement.

From optimization measurements we found that 120 images obtained from 10-frame time lapses at three different positions in four different aliquots of one urine sample are necessary to gain highly reproducible results (<5% coefficient of variation of three repeated measurements for 20 individuals, data not shown). Urine samples were aliquoted at 200 μl/well in Ibidi μ-slide

eight-well plates (Ibidi GmbH). All images were taken 300 μm above the bottom glass.

To count the number of black carbon particles in the time frames of each urine sample, a peak-find algorithm in Matlab 2010 (MathWorks, Eindhoven, the Netherlands) was used. A detailed description of the function of the customized Matlab routine can be found in the online supplement.

Validation Experiments of Optimized Urinary Carbon Load Technique

The optimized technique for measuring carbon load in urine was validated by spiking urine with known concentrations of carbon black nanopowder (US Research Nanomaterials, Houston, TX) and by analyzing the repeatability of urinary carbon load (*see* online supplement for details).

Repeatability of urinary carbon load was assessed by calculating the coefficient of variation of urine samples taken at three different time points (± 1 mo from each other; n = 19) and analyzed using the optimized experimental protocol.

Urinary Carbon Load and Real-Life Exposure to Combustion-related Air Pollution in Children

Study population and sample collection. We conducted this study in the framework of the COGNAC (Cognition and Air Pollution in Children) study, which enrolled children (aged 9–12 yr) from three different primary schools (Tienen, Zonhoven, Hasselt) in Flanders, Belgium (4). In total, we invited 770 children of which 334 children participated (43%) to the study between January 2012 and February 2014. Parents were asked to fill out a questionnaire to get additional lifestyle information of the mother's education (up to high school diploma to college or university degree) and exposure to passive tobacco smoke, and child's ethnicity, residence, transportation from and to the school, general health, state of mind, and physical activity. Written informed consent was obtained from the parents and oral consent from the children. The study protocol was approved by the ethical committees of Hasselt University and East-Limburg Hospital, Belgium. Spot urine samples (available for 289 children) were collected on the first examination day using designated metal and black carbon-free sample jars (Yvsolab, Turnhout, Belgium) and placed at 4°C until chronic storage at −80°C. To avoid external contamination from carbon particles, we aliquoted urine samples in a clean room with filtered air (Genano310; Genano OY, Espoo, Finland). Osmolality of urine was measured by the advanced Cryptomatic Osmometer (Fiske, Norwood, MA).

Residential exposure estimates. We constructed estimates of ambient exposure (black carbon, nitrogen dioxide [NO_2], and PM ≤2.5 μm [$PM_{2.5}$]), based on their residential addresses, using a spatial temporal interpolation method (18). The interpolation method uses land cover data obtained from satellite images (CORINE land cover data set) and pollution data of fixed monitoring stations. Coupled with a dispersion model (14) that uses emissions from point sources and line sources, this model chain provides daily exposure values in a high-resolution receptor grid. Overall model performance was evaluated by leave-one-out cross-validation including 14 monitoring points for black carbon, 44 for NO_2, and 34 for $PM_{2.5}$. Validation statistics of the interpolation tool gave a spatiotemporal explained variance of more than 0.74 for black carbon (19), 0.78 for NO_2 (20), and 0.80 for $PM_{2.5}$ (20). We calculated different exposure windows by averaging daily concentrations over a period preceding the examination day (i.e., recent exposure, 1 d and 1 wk before urine sampling; medium-term exposure, 1 mo before sampling; and chronic exposure, 1 and 2 yr before sampling). When a child had more than one residential address at the moment of the study, we calculated a weighted average using the proportion of time spent at each location as weights. In addition, we also calculated the residential proximity to major roads, defined as highways and other national roads (a road with more than 10,000 motor vehicles/d), using geographic information system functions (ArcGIS 9.3; Esri BeLux S.A., Wemmel, Belgium).

Statistical Analyses

Statistics were performed using SAS version 9.3 (SAS Institute Inc., Cary, NC). Partial Pearson correlation coefficients were calculated to evaluate the correlations between urinary carbon load and recent, medium-term, or chronic exposure to black carbon, NO_2, and $PM_{2.5}$ as well as residential proximity to major roads (living twice as close to major roads). To improve normality of the distributions we log-transformed residential proximity to major roads. Multiple linear regressions were performed to assess the independent associations between urinary carbon load and recent, medium-term, chronic exposure, or residential proximity to major roads, while accounting for person-related factors, including age, sex, and body mass index (BMI) of the child, mother's education, and urinary osmolality and a time-related factor, including month of examination. Results were presented as a change in urinary carbon load (particles/ml urine) for an interquartile range (IQR) increment in recent, medium-term, or chronic exposure, living twice as close to the nearest major road.

In a sensitivity analysis, we evaluated whether osmolality, creatinine, education of father (up to high school diploma to college or university degree), occupation of either parents (unemployed or not qualified worker to qualified worker, white-collar assistant, or teaching staff to self-employed, specialist, or member of management), exposure to passive smoke (none to ≤10 cigarettes/d to >10 cigarettes/d), physical activity (h/wk), or vegetable/fruit intake from own garden (percentage) affects the association between urinary carbon load and residential black carbon exposure. Additionally, we also checked the independence of recent and chronic residential black carbon exposure on urinary carbon load.

Finally, we calculated the ability to predict child's residential black carbon exposure based on the urinary carbon load. For this purpose, we estimated sensitivity and specificity of the prediction using receiver operating characteristic (ROC) plots. Children were stratified according to their chronic residential black carbon exposure with the 75th percentile as cutoff point (1.64 $\mu g/m^3$).

Results

Calibration, Optimization, and Validation of the Label-Free Optical Detection of Carbon Particles in Urine

From the calibration and optimization experiments, we arrived at the following results. (*1*) The employed detection technique is very specific for the detection of carbon particles in urine and does not detect other types of carbonaceous or noncarbonaceous particles by cross-reactivity, as shown by silica nanoparticles and carbon nanotubes (for a detailed

description, *see* online supplement, NOTE 1). Furthermore, no background signal could be observed from the artificial urine solution. (*2*) Raman fingerprints of aggregates found in dried urine samples are identical to the fingerprint of carbon-based reference particles (*see* Figure E1 in the online supplement). (*3*) Protocol parameters, such as the optimal detection plane and measurement repetition rate, were optimized to minimize the intrasample variation. A flowchart of the optimized protocol is depicted in Figure 1. The optimized experimental protocol was validated by measuring and analyzing artificial urine spiked with increasing concentrations (0–120 μg/ml) of carbon black nanopowder. A linear relation was observed ($R^2 = 0.98$) between the amount of added and detected carbonaceous particles (*see* Figure E2). Black carbon particle detection in urine by femtosecond pulsed laser microscopy is visualized in Figure 2. Repeatability of spot urine samples taken at

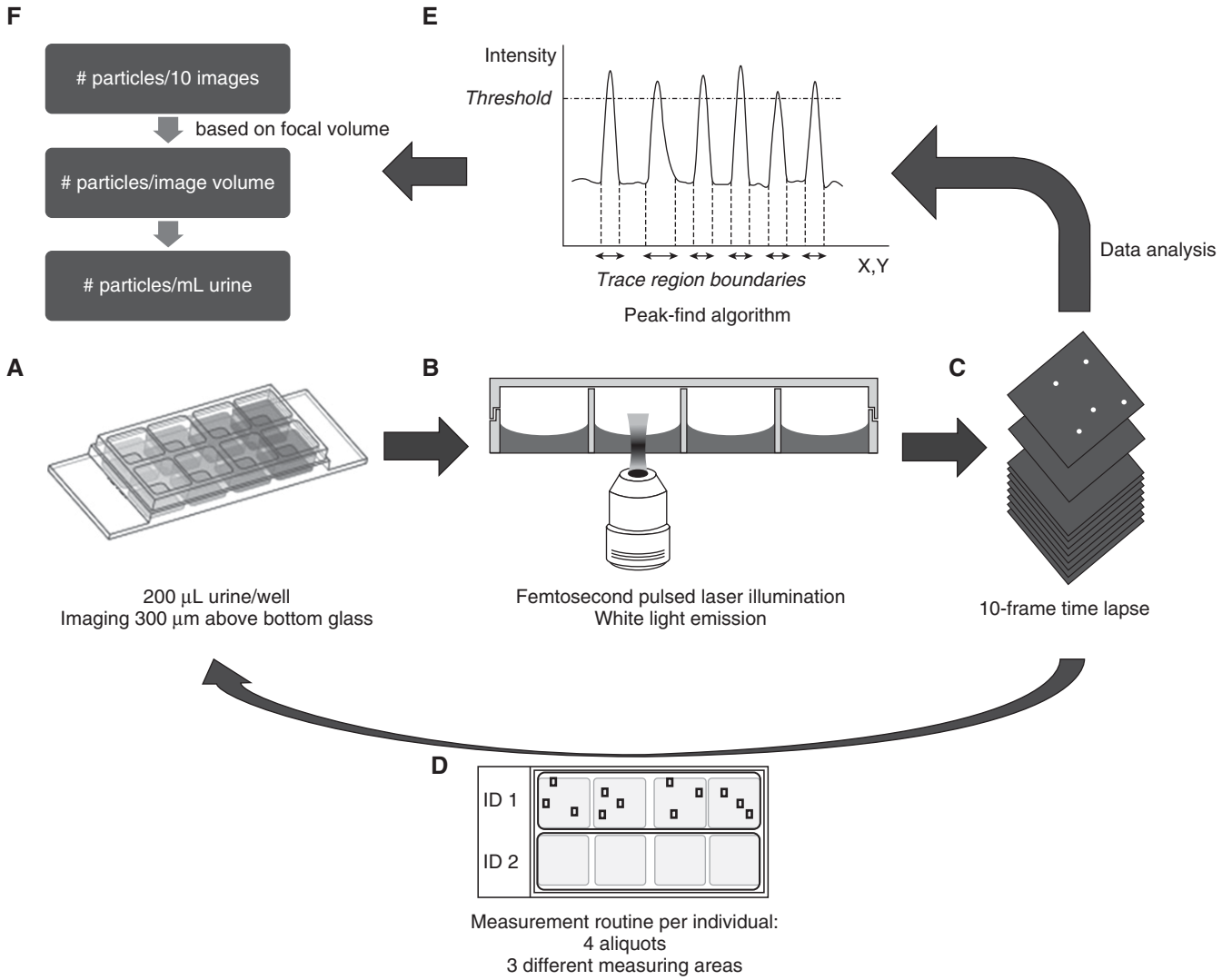

Figure 1. Flowchart of the optimized experimental protocol for black carbon detection in urine. (*A*) Each urine sample is aliquoted at 200 μl/well in an Ibidi μ-slide eight well, and images are taken 300 μm above the bottom glass of the well plate. (*B*) The samples are illuminated using a two-photon femtosecond pulsed laser tuned to a central wavelength of 810 nm (~9.7 mW radiant power at the sample position), and the white light generated by the black carbon particles naturally present in the urine is detected via analog photomultiplier detection in epi-configuration in nondescanned mode using a 40 × /1.1 water immersion objective at room temperature. (*C*) Ten consecutive images are taken on one identical location in the same well. The resulting images have a field of view of 225 × 225 μm^2 with a 512 × 512 pixel resolution (0.44 × 0.44 μm^2 pixel size) and a pixel dwell time of 3.2 μs. (*D*) In total, 120 images are obtained by recording 10-frame time lapses at three different locations in four different aliquots of one individual (ID) resulting in highly reproducible results (<5% coefficient of variation). (*E*) To determine the number of black carbon particles in the images, a peak-find algorithm counting connected pixels above a threshold value (15% lower than the highest intensity value) was used. The average amount of particles detected in the different time lapses is normalized to the image volume using the focal volume estimated from the point spread function of the optical system. (*F*) Finally, the result is expressed as the total relative number (i.e., the number of detected black carbon particles per milliliter urine). All images of each individual are analyzed in this way to retrieve a number of detected black carbon particles per milliliter urine sample.

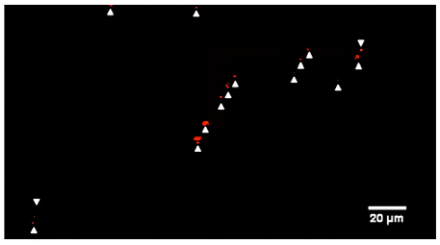

Figure 2. Black carbon particles in urine. Black carbon particles and aggregates (*arrowheads*) visualized by femtosecond pulsed laser excitation at 810 nm and observation at 400–410 nm.

three different time points (± 1 mo from each other; n = 19) showed an average coefficient of variation of 20%.

Urinary Carbon Load and Residential Black Carbon Exposure

Demographic and lifestyle characteristics are presented in Table 1. Children (50.5% boys) were on average (SD) 10.3 (1.2) years old. The distribution over mother's low and high educational class was 116 (40.1%) and 173 (59.9%), respectively. The children's BMI was 17.4 (2.9). Median (IQR) modeled exposures of black carbon, $PM_{2.5}$, and NO_2 over various time windows of exposure ranging from recent exposure (1 d and 1 wk before urine sampling), medium-term exposure (1 mo before urine sampling), and chronic exposure (1 and 2 yr before urine sampling) and median distance (IQR) from residence to major roads are given in Table 2 and Table E1. The Pearson correlation coefficient between chronic (1 yr) and recent (1 d and 1 wk) residential black carbon exposure was 0.15 (95% confidence interval [CI], 0.04–0.26) and 0.09 (95% CI, −0.03 to 0.20), respectively. The corresponding correlation between chronic and medium-term (1 mo) residential black carbon exposure was 0.36 (95% CI, 0.26–0.46).

Urinary black carbon load averaged (IQR) 98.2×10^5 (29.8×10^5) particles/ml urine (Table 1) and did not differ between boys and girls ($P = 0.55$). There was no association between urinary carbon load and child's age ($P = 0.74$), weight ($P = 0.81$), height ($P = 0.99$), BMI ($P = 0.90$), education of the mother (low vs. high: $+2.25 \times 10^6$; 95% CI, -3.38×10^5 to 7.89×10^5; $P = 0.14$), education of the father (low vs. high: $+1.61 \times 10^5$; 95% CI, -3.87×10^5 to 7.10×10^5; $P = 0.10$), highest occupation of either parents (low vs. high: $+8.83 \times 10^5$; 95% CI, -1.28×10^5 to 1.89×10^5; $P = 0.14$), physical activity ($P = 0.48$), exposure to passive smoking ($P > 0.43$), and vegetable or fruit from own garden, ($P = 0.77$). Osmolality was significantly associated with urinary carbon load (i.e., $+3.1 \times 10^5$ particles/ml [95% CI, 0.22×10^4 to 6.1×10^5] for an IQR increment in osmolality [229 mOsm/kg]), whereas urinary creatinine concentration was not a predictor of the urinary carbon load ($P = 0.82$).

Both before (Figures 3A and 3B) and after adjustment (Figure 3B) for *a priori* chosen covariates including sex, age, BMI, mother's education, month of examination, and urinary osmolality, carbonaceous particles in urine were positively correlated to medium-term black carbon exposure (partial $r = 0.12$; 95% CI, −0.002 to 0.23), chronic annual residential black carbon (partial $r = 0.17$; 95% CI, 0.05–0.28), and residential proximity to the nearest major road (partial $r = 0.15$; 95% CI, 0.03–0.26). The corresponding results for an IQR increment of medium-term black carbon and chronic annual residential black carbon exposure were $+5.90 \times 10^5$ particles/ml (95% CI, -0.81×10^4 to 11.9×10^5) and $+5.33 \times 10^5$ particles/ml (95% CI, 1.56×10^5 to 9.10×10^5) more urinary carbonaceous particles, respectively. Furthermore, children living close to a major road (first tertile: ≤160 m or median: ≤330.6 m) had 7.29×10^5 particles/ml (95% CI, 1.12×10^5 to 13.5×10^5; $P = 0.02$) or 8.78×10^5 particles/ml (95% CI, 3.14×10^5 to 14.4×10^5; $P = 0.0024$) higher urinary carbon load, respectively, compared with those living further away (>160 m or >330.6 m). Correspondingly, living twice as close to the nearest major road was associated with $+2.02 \times 10^5$ particles/ml (95% CI, 4.09×10^4 to 3.64×10^5) higher urinary carbon load. In addition, similar patterns were found for medium-term to chronic annual residential NO_2 and chronic annual $PM_{2.5}$ exposure (*see* Figure E3). All recent exposure time windows (1 d and 1 wk) of black carbon, NO_2, and $PM_{2.5}$ were not

Table 1. Characteristics of the Participants (n = 289)

Anthropometric characteristics	
Boys	143 (50.5%)
Age, yr	10.3 (1.2)
Body mass index, kg/m^2	17.4 (2.9)
Weight, kg	37.0 (9.6)
Length, cm	145 (1.0)
Lifestyle characteristics	
Mother's education	
Up to high school diploma	116 (40.1)
College or university diploma	173 (59.9)
Father's education*	
Up to high school diploma	132 (47.3)
College or university diploma	147 (52.7)
Most prestigious category of occupation of either parent	
Unemployed or not qualified worker	23 (7.9)
Qualified worker, white-collar assistant, or teaching staff	118 (40.8)
Self-employed, specialist, or member of management	148 (51.2)
Exposure to passive tobacco smoke	
None	263 (78.3)
≤10 cigarettes/d	44 (13.1)
>10 cigarettes/d	29 (8.6)
Physical activity, h/wk	3.3 (2.4)
Urinary characteristics	
Osmolality, mOsm/kg	927.9 (212.3)
Creatinine, mg/dl†	127.0 (48.9)
Carbon load, particles/ml	98.2×10^5 (29.8×10^5)

Arithmetic mean (SD) is given for the continuous variables. Number (%) is given for the categorical variables.
*Data available for 279 participants.
†Data available for 276 participants.

Table 2. Residential Exposure Characteristics (n = 289)

Residential Exposure	Median	25th Percentile	75th Percentile
Recent black carbon, μg/m^3			
1 d	1.45	1.19	2.23
1 wk	1.68	1.27	2.27
Medium-term black carbon, μg/m^3			
1 mo	1.63	1.38	1.83
Chronic black carbon, μg/m^3			
1 yr	1.54	1.43	1.64
2 yr	1.53	1.43	1.65
Distance to major roads, m	330.60	126.70	820.40

correlated with the carbonaceous particles in urine.

Sensitivity analysis showed a robust association between urinary carbon load and residential, annual black carbon exposure with and without adjustment for osmolality, with replacing osmolality by creatinine or by adjusting for both osmolality and creatinine as measures of urine concentration (*see* Table E2). Furthermore, no changes were observed when the main model with *a priori* chosen covariates was additionally adjusted for education of the father, highest occupation of either parents, exposure to passive smoking, physical activity, creatinine, or vegetable/fruit intake from own garden (*see* Table E2). Furthermore, we also showed independence of the recent and chronic residential exposure on the internal urinary carbon load (*see* Table E2).

Finally, Figure 4 shows the ROC curve analysis with sensitivity and one minus specificity (false-positive ratio) of chronic residential black carbon exposure (75th percentile as cutoff point, 1.64 μg/m^3) in association with children's urinary carbon load. The model adjusted for aforementioned *a priori* chosen covariates had an area under the curve value of 0.74 (95% CI, 0.67–0.81).

Discussion

In the prospect that ultrafine particles may translocate in the circulation and be cleared into the urine, we developed a method to measure urinary black carbon load as an exposure matrix of carbonaceous particles in a population at fairly low exposure levels, more specifically in children as a susceptible subgroup for the detrimental effects of air pollution. Overall, our results demonstrate the use of white-light generation of black carbon particles in urine under femtosecond pulsed laser illumination as a measure for exposure to combustion-related black carbon air pollution. The novel information from our work comprises the following: (*1*)

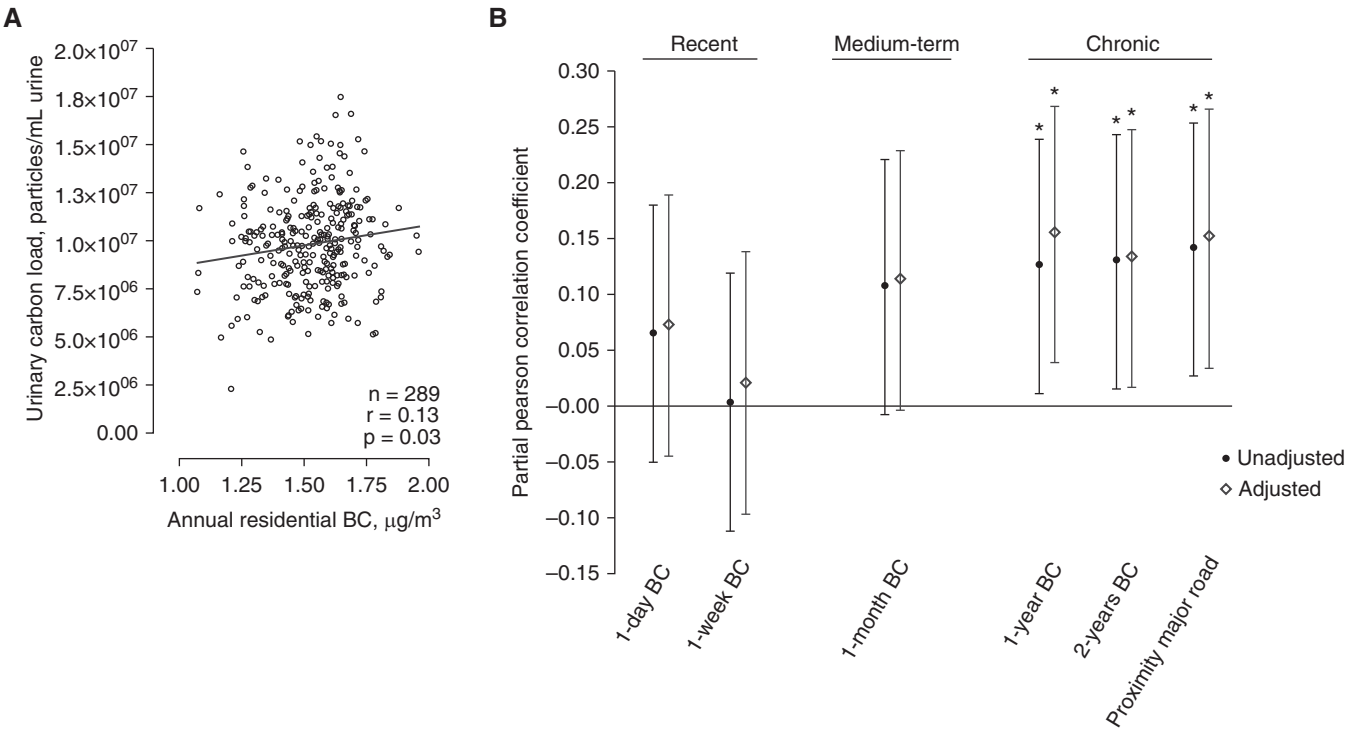

Figure 3. Correlation between urinary black carbon load and residential exposure to recent (1 d, 1 wk) up to chronic (1 yr, 2 yr) black carbon or proximity to major roads. (*A*) Dose–response relationship between urinary black carbon load and annual residential black carbon exposure, adjusted for urinary osmolality. The *line* is the regression line. (*B*) Unadjusted and partial Pearson correlation coefficient and 95% confidence intervals between urinary black carbon load and residential recent (1 d and 1 wk before urine sampling), medium-term (1 mo before urine sampling), or chronic (1 and 2 yr before urine sampling) black carbon exposure or residential proximity to major roads ($\log_{10}$). Partial correlation coefficients were adjusted for *a priori* chosen covariates including sex, age, body mass index, mother's education, month of examination, and urinary osmolality. *$P < 0.05$. BC = black carbon.

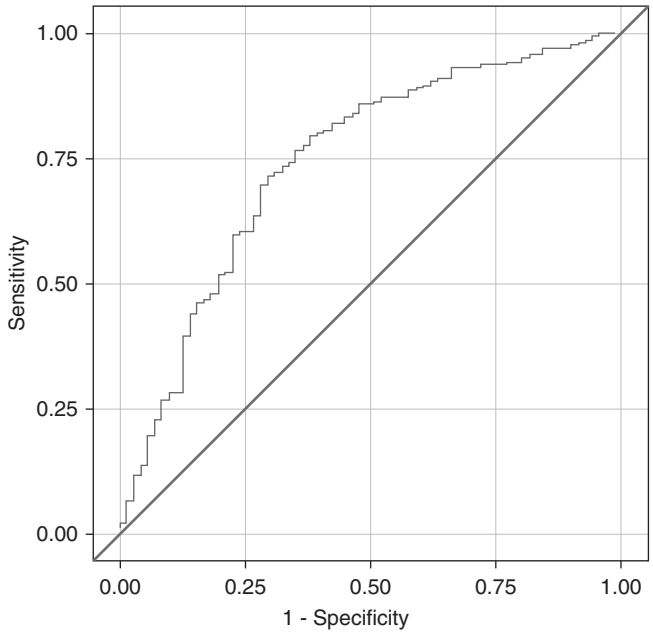

Figure 4. Receiver operating characteristics curve for urinary carbon load distinguishing between high and low residential black carbon exposure. Performance of urinary carbon load to differentiate between high (>75th percentile: 1.64 $\mu g/m^3$) and low ($\leq$1.64 $\mu g/m^3$) exposure to chronic residential black carbon exposure. The model was adjusted for sex, age, body mass index, mother's education, month of examination, and urinary osmolality.

urinary black carbon load mirrors medium-term to chronic ambient exposure, even at low environmental concentrations; (*2*) our method requires no additional labeling or preparation procedure and the raw data can be analyzed using a simple peak-find algorithm; and (*3*) detection of black carbon particles in urine reflects the passage of black carbon particles from the circulation into the urine.

Different experimental rat studies have demonstrated that ultrafine particles can translocate from the lung into the circulation (21, 22). These particles can accumulate at sites of vascular inflammation (23) and have direct access to intracellular compartments, such as proteins, organelles, and DNA (22). Furthermore, Oberdörster and coworkers (12) demonstrated that intranasally instilled solid ultrafine particles translocate along axons of the olfactory nerve into the central nervous system. In this regard, Maher and coworkers (24) recently identified the presence of magnetite nanoparticles, formed by combustion- and/or friction-derived heating in the human brain. Suggested pathways for particle translocation into the circulation are either across the alveolar epithelium or across the intestinal epithelium from particles that have been cleared via mucous ingested into the gastrointestinal tract (12). Nevertheless, the issue of particle translocation in humans is still controversial. Nemmar and coworkers (25) showed that inhaled technetium-99m-labeled ultrafine carbon particles could rapidly pass into the systemic circulation.

Other studies, however, using short-term inhalation (up to 2 d) of technetium-99m-labeled ultrafine carbon particles found that most of the inhaled particles were retained in the lung periphery and in the conducting airways without substantial translocation to the systemic circulation (26–28). Mills and coworkers (26) reported that the radioactive moiety of the label, rather than the particle itself, was detected in the blood. Wiebert and colleagues (27) found no significant translocation of inhaled 35-nm carbon particles to the circulation in humans. Another study (29) on pulmonary deposition and retention of indium-111-labeled ultrafine carbon particles in healthy individuals only found marginal translocation of particles from lungs to blood (0.3%). Moreover, there was no observable elimination of particles from the body via urine 1 week postadministration. These studies, which are based on labeling techniques and short-term exposure conditions, contrast with our current findings using label-free white-light detection of urinary black carbon in children continuously exposed to low levels of air pollution as in real life.

Because of the stability of inhaled ultrafine carbon particles, long-term retention in the human lung is expected and may accumulate to a chronic particle load (28). In this regard, Churg and Brauer (30) observed that large quantities of fine and ultrafine aggregates retain in the human lung parenchyma whereby ultrafine particles make up only a small fraction of the retained total (31). Furthermore, a recent study showed that circulation levels of 5-nm gold particles were greater compared with inhaled 30-nm particles (23). The smallest particles are in steady state because they are retained longer with potential translocation mechanisms from the lungs to the system (12, 28). This is in line with our observations that residential medium-term to chronic ambient black carbon concentrations are significantly associated with urinary black carbon load. In contrast to our method, labeling studies are not able to detect the background load of particles in urine.

In the past, efforts have been made to identify a reliable and effective biomarker for combustion-related exposure. Oxidative stress is considered as one of the mechanisms through which traffic-related air pollution exerts its effects on human health. The urinary excretion of 8-oxo-7,8-dihydro-2-deoxyguanosine is used as a biomarker of response to evaluate the prooxidant effects of vehicle exhaust emissions on DNA (32). Another example is the metabolite of benzene, urinary trans, trans muconic acid (*t,t*-MA), which has been considered as a proxy-biomarker for traffic (33, 34). However, the aforementioned biomarkers are not specifically related to combustion-associated air pollution. Furthermore, these biomarkers do not reflect chronic exposure. More recently, carbon load in alveolar macrophages has been used as a biomarker of exposure to traffic exhaust pollution and biomass smoke exposure (35, 36). However, this technique requires semiinvasive sampling procedures (sputum induction) with success rates of approximately 60% (36, 37), and identified black carbon particles using light microscopy, thereby

underestimating the total amount of carbon load (35). Our current technique to detect carbon load in urine does not require invasive sampling procedures and uses label-free white-light generation detection to determine the amount of black carbon particles in urine, a technique specifically to detect carbonaceous particles. Aside from continuous analysis, we established ROC curves to separate residential chronic low (75th percentile) exposed from higher exposed children for black carbon and showed an area under de curve of 0.74. Therefore, our novel exposure biomarker has the ability to distinguish between true- and false positives.

We acknowledge some limitations of our study. First, ambient black carbon particles in the air could have contaminated the urine samples. By using a clean room with filtered air to handle the urine samples and using sterile metal-free collection tubes, we avoid potential external contamination of carbon particles. Furthermore, no background signals from naturally present carbonaceous particles in the air were observed in the detection chambers or in the sterile metal-free collection tubes. Second, we cannot exclude that black carbon particles detected in urine might mirror particles entered through food or drinks, or even uptake through skin instead of translocation from the lung to the system. However, in our sensitivity analysis, consuming vegetables or fruit from one's own garden did not predict the carbon load in urine. Third, urban air consists of particles with a size between 0.02 and 100 μm, with primary particle size ranging from 6 to 100 nm (38). Diesel particles usually consist of aggregates with a diameter of 10–40 nm (39). Particles with a diameter up to 75 nm may diffuse and accumulate in the mesangium of the glomerulus (40). The glomerular filtration instigates renal clearance of particles with a size of 10 nm and smaller (40). Although it is possible to detect the smallest particles present in the urine it is not possible to determine their size and distribution because of the diffraction limit in optical microscopy. Fourth, our external exposure estimates of black carbon relates to modeled residential exposure, and not to personal monitoring. Measurement via personal exposure samplers is not practical to assess long-term exposure of large population samples. Validation statistics of the exposure model showed an explained spatiotemporal variance of greater than 0.74 for black carbon.

In conclusion, we showed for the first time that urinary black carbon load in children is associated with medium-term to chronic exposure to ambient combustion-related pollution. This specific biomarker reflects internal systemic black carbon particles providing its utility to unravel the complexity of particulate-related health effects, and can be used in different study populations over the entire life course. ■

Author disclosures are available with the text of this article at www.atsjournals.org.

Acknowledgment: The authors thank Mr. E. Slenders for designing the analysis software in Matlab 2010 (MathWorks).

References

1. Collaborators GBDRF; GBD 2015 Risk Factors Collaborators. Global, regional, and national comparative risk assessment of 79 behavioural, environmental and occupational, and metabolic risks or clusters of risks, 1990-2015: a systematic analysis for the Global Burden of Disease Study 2015. *Lancet* 2016;388:1659–1724.
2. Pedersen M, Giorgis-Allemand L, Bernard C, Aguilera I, Andersen AM, Ballester F, Beelen RM, Chatzi L, Cirach M, Danileviciute A, *et al*. Ambient air pollution and low birthweight: a European cohort study (ESCAPE). *Lancet Respir Med* 2013;1:695–704.
3. Sunyer J. The neurological effects of air pollution in children. *Eur Respir J* 2008;32:535–537.
4. Saenen ND, Provost EB, Viaene MK, Vanpoucke C, Lefebvre W, Vrijens K, Roels HA, Nawrot TS. Recent versus chronic exposure to particulate matter air pollution in association with neurobehavioral performance in a panel study of primary schoolchildren. *Environ Int* 2016;95: 112–119.
5. Colicino E, Wilson A, Frisardi MC, Prada D, Power MC, Hoxha M, Dioni L, Spiro A, Vokonas PS, Weisskopf MG, *et al*. Telomere length, long-term black carbon exposure, and cognitive function in a cohort of older men: the VA Normative Aging Study. *Environ Health Perspect* 2017;125: 76–81
6. Nawrot TS, Perez L, Künzli N, Munters E, Nemery B. Public health importance of triggers of myocardial infarction: a comparative risk assessment. *Lancet* 2011;377:732–740.
7. Brook RD, Rajagopalan S, Pope CA III, Brook JR, Bhatnagar A, Diez-Roux AV, Holguin F, Hong Y, Luepker RV, Mittleman MA, *et al*.; American Heart Association Council on Epidemiology and Prevention, Council on the Kidney in Cardiovascular Disease, and Council on Nutrition, Physical Activity and Metabolism. Particulate matter air pollution and cardiovascular disease: an update to the scientific statement from the American Heart Association. *Circulation* 2010;121: 2331–2378.
8. Guerra S, Halonen M, Vasquez MM, Spangenberg A, Stern DA, Morgan WJ, Wright AL, Lavi I, Tarès L, Carsin AE, *et al*. Relation between circulating CC16 concentrations, lung function, and development of chronic obstructive pulmonary disease across the lifespan: a prospective study. *Lancet Respir Med* 2015;3:613–620.
9. Raaschou-Nielsen O, Andersen ZJ, Beelen R, Samoli E, Stafoggia M, Weinmayr G, Hoffmann B, Fischer P, Nieuwenhuijsen MJ, Brunekreef B, *et al*. Air pollution and lung cancer incidence in 17 European cohorts: prospective analyses from the European Study of Cohorts for Air Pollution Effects (ESCAPE). *Lancet Oncol* 2013;14:813–822.
10. Pieters N, Plusquin M, Cox B, Kicinski M, Vangronsveld J, Nawrot TS. An epidemiological appraisal of the association between heart rate variability and particulate air pollution: a meta-analysis. *Heart* 2012; 98:1127–1135.
11. Shimada A, Kawamura N, Okajima M, Kaewamatawong T, Inoue H, Morita T. Translocation pathway of the intratracheally instilled ultrafine particles from the lung into the blood circulation in the mouse. *Toxicol Pathol* 2006;34:949–957.
12. Oberdörster G, Sharp Z, Atudorei V, Elder A, Gelein R, Kreyling W, Cox C. Translocation of inhaled ultrafine particles to the brain. *Inhal Toxicol* 2004;16:437–445.
13. Beelen R, Raaschou-Nielsen O, Stafoggia M, Andersen ZJ, Weinmayr G, Hoffmann B, Wolf K, Samoli E, Fischer P, Nieuwenhuijsen M, *et al*. Effects of long-term exposure to air pollution on natural-cause mortality: an analysis of 22 European cohorts within the multicentre ESCAPE project. *Lancet* 2014;383:785–795.
14. Lefebvre W, Degrawe B, Beckx C, Vanhulsel M, Kochan B, Bellemans T, Janssens D, Wets G, Janssen S, de Vlieger I, *et al*. Presentation and evaluation of an integrated model chain to respond to traffic- and health-related policy questions. *Environ Model Softw* 2013;40: 160–170.
15. Sheppard L, Burnett RT, Szpiro AA, Kim SY, Jerrett M, Pope CA III, Brunekreef B. Confounding and exposure measurement error in air pollution epidemiology. *Air Qual Atmos Health* 2012;5:203–216.
16. Bové H, Steuwe C, Fron E, Slenders E, D'Haen J, Fujita Y, Uji-I H, vandeVen M, Roeffaers M, Ameloot M. Biocompatible label-free detection of carbon black particles by femtosecond pulsed laser microscopy. *Nano Lett* 2016;16:3173–3178.
17. Kelly A. Concise encyclopedia of composite materials. Amsterdam, the Netherlands: Elsevier Science Ltd; 2012.

18. Janssen S, Dumont G, Fierens F, Mensink C. Spatial interpolation of air pollution measurements using CORINE land cover data. *Atmos Environ* 2008;42:4884–4903.
19. Lefebvre W, Vercauteren J, Schrooten L, Janssen S, Degraeuwe B, Maenhaut W, De Vlieger I, Vankerkom J, Cosemans G, Mensink C, *et al*. Validation of the MIMOSA-AURORA-IFDM model chain for policy support: modeling concentrations of elemental carbon in Flanders. *Atmos Environ* 2011;45:6705–6713.
20. Maiheu B, Veldeman B, Viaene P, De Ridder K, Lauwaet D, Smeets N, Deutsch FSJ. Identifying the best available large-scale concentration maps for air quality in Belgium. 2012 [accessed 2016 Feb 26]. Available from: http://www.milieurapport.be/Upload/main/0_onderzoeksrapporten/2013/Eindrapport_Concentratiekaarten_29_01_2013_TW.pdf
21. Meiring JJ, Borm PJ, Bagate K, Semmler M, Seitz J, Takenaka S, Kreyling WG. The influence of hydrogen peroxide and histamine on lung permeability and translocation of iridium nanoparticles in the isolated perfused rat lung. *Part Fibre Toxicol* 2005;2:3.
22. Geiser M, Rothen-Rutishauser B, Kapp N, Schürch S, Kreyling W, Schulz H, Semmler M, Im Hof V, Heyder J, Gehr P. Ultrafine particles cross cellular membranes by nonphagocytic mechanisms in lungs and in cultured cells. *Environ Health Perspect* 2005;113:1555–1560.
23. Miller MR, Raftis JB, Langrish JP, McLean SG, Samutrtai P, Connell SP, Wilson S, Vesey AT, Fokkens PHB, Boere AJF, *et al*. Inhaled nanoparticles accumulate at sites of vascular disease. *ACS Nano* 2017;11:4542–4552.
24. Maher BA, Ahmed IA, Karloukovski V, MacLaren DA, Foulds PG, Allsop D, Mann DM, Torres-Jardón R, Calderon-Garciduenas L. Magnetite pollution nanoparticles in the human brain. *Proc Natl Acad Sci USA* 2016;113:10797–10801.
25. Nemmar A, Hoet PH, Vanquickenborne B, Dinsdale D, Thomeer M, Hoylaerts MF, Vanbilloen H, Mortelmans L, Nemery B. Passage of inhaled particles into the blood circulation in humans. *Circulation* 2002;105:411–414.
26. Mills NL, Amin N, Robinson SD, Anand A, Davies J, Patel D, de la Fuente JM, Cassee FR, Boon NA, Macnee W, *et al*. Do inhaled carbon nanoparticles translocate directly into the circulation in humans? *Am J Respir Crit Care Med* 2006;173:426–431.
27. Wiebert P, Sanchez-Crespo A, Falk R, Philipson K, Lundin A, Larsson S, Möller W, Kreyling WG, Svartengren M. No significant translocation of inhaled 35-nm carbon particles to the circulation in humans. *Inhal Toxicol* 2006;18:741–747.
28. Möller W, Felten K, Sommerer K, Scheuch G, Meyer G, Meyer P, Häussinger K, Kreyling WG. Deposition, retention, and translocation of ultrafine particles from the central airways and lung periphery. *Am J Respir Crit Care Med* 2008;177:426–432.
29. Klepczyńska-Nyström A, Sanchez-Crespo A, Andersson M, Falk R, Lundin A, Larsson BM, Svartengren M. The pulmonary deposition and retention of indium-111 labeled ultrafine carbon particles in healthy individuals. *Inhal Toxicol* 2012;24:645–651.
30. Churg A, Brauer M. Human lung parenchyma retains PM2.5. *Am J Respir Crit Care Med* 1997;155:2109–2111.
31. Brauer M, Avila-Casado C, Fortoul TI, Vedal S, Stevens B, Churg A. Air pollution and retained particles in the lung. *Environ Health Perspect* 2001;109:1039–1043.
32. Lettieri Barbato D, Tomei G, Tomei F, Sancini A. Traffic air pollution and oxidatively generated DNA damage: can urinary 8-oxo-7,8-dihydro-2-deoxiguanosine be considered a good biomarker? A meta-analysis. *Biomarkers* 2010;15:538–545.
33. Staessen JA, Nawrot T, Hond ED, Thijs L, Fagard R, Hoppenbrouwers K, Koppen G, Nelen V, Schoeters G, Vanderschueren D, *et al*. Renal function, cytogenetic measurements, and sexual development in adolescents in relation to environmental pollutants: a feasibility study of biomarkers. *Lancet* 2001;357:1660–1669.
34. Kicinski M, Vermeir G, Van Larebeke N, Den Hond E, Schoeters G, Bruckers L, Sioen I, Bijnens E, Roels HA, Baeyens W, *et al*. Neurobehavioral performance in adolescents is inversely associated with traffic exposure. *Environ Int* 2015;75:136–143.
35. Bai Y, Brugha RE, Jacobs L, Grigg J, Nawrot TS, Nemery B. Carbon loading in airway macrophages as a biomarker for individual exposure to particulate matter air pollution: a critical review. *Environ Int* 2015;74:32–41.
36. Kulkarni N, Pierse N, Rushton L, Grigg J. Carbon in airway macrophages and lung function in children. *N Engl J Med* 2006;355:21–30.
37. Jacobs L, Emmerechts J, Mathieu C, Hoylaerts MF, Fierens F, Hoet PH, Nemery B, Nawrot TS. Air pollution related prothrombotic changes in persons with diabetes. *Environ Health Perspect* 2010;118:191–196.
38. Xiong C, Friedlander SK. Morphological properties of atmospheric aerosol aggregates. *Proc Natl Acad Sci USA* 2001;98:11851–11856.
39. Shi JP, Mark D, Harrison RM. Characterization of particles from a current technology heavy-duty diesel engine. *Environ Sci Technol* 2000;34:748–755.
40. Choi CH, Zuckerman JE, Webster P, Davis ME. Targeting kidney mesangium by nanoparticles of defined size. *Proc Natl Acad Sci USA* 2011;108:6656–6661.